Eur. Phys. J. Plus (2025) 140:569
https://doi.org/10.1140/epjp/s13360-025-06502-x

THE EUROPEAN PHYSICAL JOURNAL PLUS

Regular Article

Characterization of Cr_3C_2/Ni ceramic–metal composites produced by direct resistance rapid hot pressing method

Büşra Tunç[1,a], **İlyas Somunkiran**[2,b], **Esra Balci**[3,c]

[1] Department of Control and Automation, Borçka Acarlar Vocational School, Artvin Çoruh University, Artvin, Turkey
[2] Department of Aircraft Maintenance and Repair, School of Civil Aviation, Faculty of Technology, University of Firat, Elazig, Turkey
[3] Department of Aircraft Maintenance and Repair, School of Civil Aviation, Istanbul Nisantasi University, Istanbul, Turkey

Received: 5 February 2025 / Accepted: 30 May 2025

Abstract The Cr_3C_2 phase of chromium carbides exhibits excellent corrosion resistance and low density, but vacancies in these materials sometimes limit their use in some applications. In order to expand the areas of use and further develop these materials, cermets containing metallic phases that provide better strength, hardness, and workability have been developed. This study examined the microstructure and mechanical properties of Cr_3C_2–Ni cermets fabricated through direct resistance rapid hot pressing. Cr_3C_2 and Ni powders were mixed in varying ratios, sintered, and analyzed using optical microscopy and X-ray diffraction for microstructural characterization. Mechanical properties were evaluated via Vickers hardness tests, density was measured using Archimedes' principle, and wear behavior was assessed. Results indicated that changes in Cr_3C_2 content significantly influenced mechanical properties and wear resistance, with the sample containing 18% Cr_3C_2 displaying superior strength and wear resistance. These findings highlight the potential of Cr_3C_2–Ni cermets in applications demanding robust and durable materials, representing a significant advancement in their development.

1 Introduction

In recent years, ceramic materials have attracted significant attention due to their high hardness, high melting points, and excellent mechanical properties [1]. Among the most well-known ceramic materials are Al_2O_3, WC, TiC, SiC, and Cr_3C_2 [2, 3]. Among these ceramic materials, chromium carbides exist in three forms: Cr_3C_2, Cr_7C_3, and $Cr_{23}C_6$. Especially, Cr_3C_2 possesses properties such as high strength, excellent coating resistance, low density, and good chemical stability [4]. However, during the sintering process, numerous voids are formed in ceramics. These voids limit the strength, fracture toughness, and industrial applications of the ceramics. To overcome these limitations, various metallic phases such as Co, Ni, Fe, Cu, and Mo are added to ceramic materials [5]. The composites obtained in this manner are referred to as cermets (ceramic–metal composites). Cermets are formed by the combination of ceramic particles with a metallic binder phase, and they possess common advantages such as higher hardness, strength, and exceptional machinability [6–14]. These composites exhibit lower porosity, better microstructural distribution, and superior mechanical properties [15]. Various ceramic–metal composites, such as WC–Co [16, 17], TiC–Fe [18], SiC–Cu [19, 20], and Cr_3C_2–Ni [21], have been extensively researched and utilized in industrial applications due to their excellent performance [22–24]. In addition to these, Ni- and Ni-based superalloys have been extensively studied for the preparation of ceramic–metal composites due to their good ductility and excellent high-temperature properties [1]. The close thermal expansion coefficients of Cr_3C_2 and Ni effectively prevent the formation of microcracks at the interface, thereby enhancing the bonding strength between the ceramic and metallic phases. Chromium carbide–nickel composites are widely used in aerospace engineering, automotive manufacturing, high-temperature coatings, and petrochemical environments due to their superior mechanical properties and high-temperature performance [15]. Therefore, in this study, chromium carbide and Ni were investigated as ceramic and metallic phases. Some examples of current studies are as follows: Weng et al. [5] examined the high-temperature oxidation behavior of Ni-based alloys and found that they exhibit excellent oxidation resistance due to the formation of Cr_2O_3. Klenk et al. [25] discovered that Ni-based alloys demonstrate exceptional welding behavior at high temperatures, making them suitable for applications in power plant components and turbine pipes. The thermal expansion coefficients of Cr_3C_2 and Ni are 10.3×10^{-6}/°C and 13×10^{-6}/°C, respectively, and this compatibility effectively prevents the formation of interface microcracks, thereby enhancing the bonding strength between the ceramic and metallic phases [1]. Bullock et al. [26] investigated directionally solidified Ni–Ni_3Al–Cr_3C_2

[a] e-mail: busratunc@artvin.edu.tr (corresponding author)
[b] e-mail: ilyass@firat.edu.tr
[c] e-mail: esra.balci@nisantasi.edu.tr

Published online: 23 June 2025

Table 1 Mass percentage mixing ratios and coding of the powders constituting the samples

Sample	Cr_3C_2 content (wt.%)	Ni content (wt.%)
N1	3	97
N2	6	94
N3	9	91
N4	12	88
N5	18	82

composites and found that these composites exhibited better creep resistance than the matrix material alone. The wear performance of chromium carbide-reinforced Ni_3Al matrix composites at ambient temperature has been studied by Gong et al. [27–29] Duran et al. [11] produced Cr_3C_2–NiCr composites using Cr_3C_2, Ni, and Cr mixed powders at 1573 K and found that these composites had a bending strength of approximately 600 MPa. Hussainova et al. [14] prepared chromium carbide-nickel composites using the method employed by Duran et al. [11] and added a small amount of Mo to improve the microstructure and physical properties. As a result of this method, the bending strength increased to approximately 1100 MPa, and this improvement was attributed to grain refinement and the enhancement of physical properties due to the addition of alloying elements.

With advancing technology and the increasing demand for stronger materials, the development of superalloys with complex chemical compositions containing heavy elements has become prevalent. Challenges have arisen in obtaining homogenous superalloys free of segregation through conventional ingot metallurgy [30]. To overcome these challenges, a powder metallurgy (P/M) method has been developed, which involves powder production via inert gas/vacuum atomization, powder consolidation through hot isostatic pressing (HIP)/hot extrusion, and subsequent isothermal forging [30]. Some important examples in the literature are as follows: Chang et al. [31] reported that hot isostatic pressing (HIP) eliminated casting microporosities in the nickel-based SX superalloy CMSX-4, resulting in an 185% improvement in stress-rupture life at 950 °C/355 MPa. Ruttert et al. [32] confirmed the positive effects of HIP on the porosity and low-cycle fatigue (LCF) life of the nickel-based SX superalloy ERBO/1 at high temperatures. However, the impact of HIP on the tensile properties of SX superalloys has been rarely reported, as microporosity is not commonly considered a major factor influencing failure during tensile deformation. Recently, Fritzemeier et al. [33] and Razumovskii et al. [33] found that HIP enhances the ductility of the SX superalloys PWA1480 and GS32 at ambient temperature.

In this study, high-density homogeneous composite materials were obtained by using the direct resistance rapid hot pressing technique method in order to provide lower energy consumption with a shorter production process. This method provided significant advantages in improving the microstructure and mechanical properties compared to the conventional HIP (hot isostatic pressing) method. The microstructure and phase composition of Cr_3C_2/Ni composites were characterized using optical microscopy and X-ray diffraction (XRD) techniques. Additionally, microhardness and density measurements were conducted, and the obtained data were evaluated. The wear behaviors were also analyzed in detail and interpreted.

2 Experimental procedure

Firstly, in the study, commercially pure Cr_3C_2 (99.9% purity, supplied by Alfa Aesar, Thermo Fisher Scientific, USA) and Ni (99.9% purity, supplied by Sigma-Aldrich, USA) powders were used. Ni powder was used as the matrix and Cr_3C_2 powder at different weight percentages (3%, 6%, 9%, 12%, 18%) was used as the reinforcement. To achieve a homogeneous mixture, the prepared powder mixtures were mixed in a three-axis mixer at 180 rpm for 60 min. Three samples from each group were produced for microstructural, XRD, and wear analyses. The mass percentage mixing ratios and coding of the powders constituting the samples are given in Table 1. Subsequently, the powder mixtures were placed into graphite molds with dimensions of $40 \times 10 \times 7$ mm^3 and sintered at 960 °C under 35 MPa pressure for 6 min using a direct resistance hot pressing device (HPV 120, ÇELMAK Machine Industry and Trade Limited Company, Turkey).

Liquid boron nitride was applied to the graphite mold to prevent the sample from sticking to the mold and to prevent mass loss. Additionally, an N_2 gas atmosphere was used during the sintering process to prevent samples from coming into contact with oxygen. After the hot pressing process, microstructural analyses were performed on the prepared samples by sequential grinding with 240–1200-grit SiC sandpapers. After grinding, the samples were polished using a 3 μm diamond solution and ethanol. To facilitate microstructural analysis, the samples were then chemically etched with 5% HNO_3 + 95% C_2H_5OH solution.

Microstructural analyses of the samples were carried out using an optical microscope (Nikon Eclipse MA200, Nikon Corporation, Japan). To analyze phase transformations in the produced Ni-based cermet samples, an X-ray diffractometer (Rigaku RadB-DMax II, Rigaku Corporation, Japan) was used. The XRD analysis was performed with $Cu_{K\alpha}$ radiation ($\lambda = 1.54059$ Å) over a scanning range of 20°–90°. In addition to microstructural analysis, the hardness values of the cermet samples were determined using the Vickers hardness measurement technique with a microhardness tester (Emcotest Duroscan G5, EMCO-TEST Prüfmaschinen GmbH, Austria) to assess their mechanical properties. Hardness values were determined by taking measurements from five different points on each sample and calculating the arithmetic mean of the results. Archimedes' principle was used to determine the density changes in the

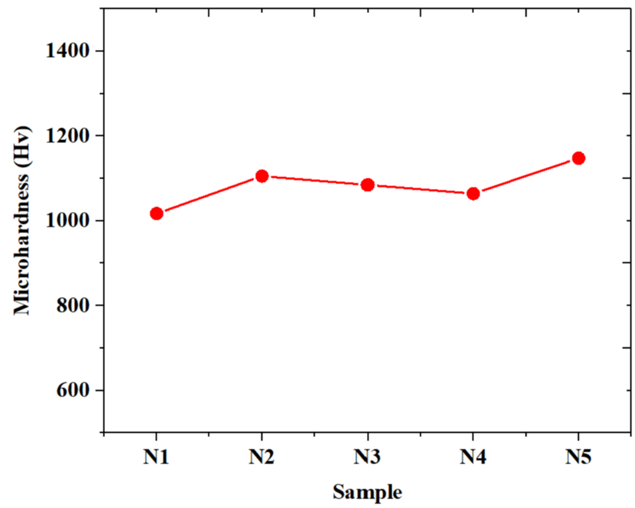

Fig. 1 Microhardness analysis graph of samples taken by Vickers method

cermets after sintering (Eq. 1). In this equation (Eq. 1), D is the density of the sample, W_{air} is the dry weight of the sample in air, W_{water} is the weight of the sample in water, and ρ_{water} is the density of the water used. The density measurements of the produced samples were performed using a precision electronic balance (GR-200, A&D Company, Ltd., Japan) with a sensitivity of 0.001 g. For measurements before and after wear tests, the mass of the samples was determined using the precision balance. The amount of wear was calculated by examining the difference between these two weights (Eq. 2). The dry weights of the samples were first determined, followed by measuring their weights again in a container filled with pure water at a measured temperature.

$$D = \frac{W_{\text{air}}}{W_{\text{air}} - W_{\text{water}}} \times \rho_{\text{water}} \tag{1}$$

$$V = \text{Wear trace} \times \text{Sliding distance} \tag{2}$$

$$\Delta W = V \times \rho$$

V = The volume of wear, ρ = Material density.

For some mechanical characterization of the samples, the wear test was performed using a tribometer T10/20 device in a pin-on-disk configuration. In the tests, a Ø6-mm-diameter Al_2O_3 ball was used. During the wear test, a load of 20 N was applied, the sliding distance was set to 300 m, and the sliding speed was fixed at 300 rpm. After the wear tests, optical microscope analyses were conducted to examine the worn surfaces of the samples and determine the wear mechanisms. It is well known that microstructural images are essential to examine the surface morphology changes and microstructural features that occur during the wear process. The tribometer T10/20 device is an advanced testing equipment that enables precise and repeatable wear tests. Its high-precision load and speed control enhance the reliability and accuracy of the wear tests.

3 Results and discussion

As is well known, the addition of Cr_3C_2 in Ni-based cermets significantly influences their microstructure and mechanical properties. In this study, Ni-based cermets containing varying amounts of Cr_3C_2 were prepared to determine the optimal addition ratio. Microhardness measurement results of the samples are given in Fig. 1. According to these results, increasing the amount of chromium carbide led to notable changes in the density of the Ni-based cermets. These changes are attributed to the differing density of Cr_3C_2 compared to Ni, which is thought to affect the overall density of the composite directly. Therefore, the increased Cr_3C_2 content also influenced the porosity level and internal structural integrity of the material, resulting in the observed variations in density. Figure 2 shows the graph of density measurements of the samples before the wear analysis. Microhardness measurements show a significant increase in the hardness values of Ni-based cermets with the rising Cr_3C_2 addition ratio. The microhardness measurement yielded 1017.5 HV for N1 and 1147.6 HV for N5. This increase is attributed to the incorporation of Cr_3C_2's hard and wear-resistant structure into the Ni matrix. Consequently, the addition of Cr_3C_2 in specific ratios significantly enhanced the mechanical strength and wear resistance of the Ni-based cermets.

The increase in chromium carbide content generally led to a rise in the density of the samples, indicating a more compact structure. This densification trend, particularly observed at lower Cr_3C_2 additions, suggests a reduction in porosity, which in turn resulted in an increase in microhardness values (Fig. 1). However, when the Cr_3C_2 content was increased from 3 to 6%, a slight decrease in density was recorded, although the microhardness continued to increase. This behavior can be attributed to the higher fraction of the chromium carbide phase, which possesses significantly greater hardness. In this system, where nickel acts as the binder and matrix

Fig. 2 Graph of density measurements of the samples before the wear analysis

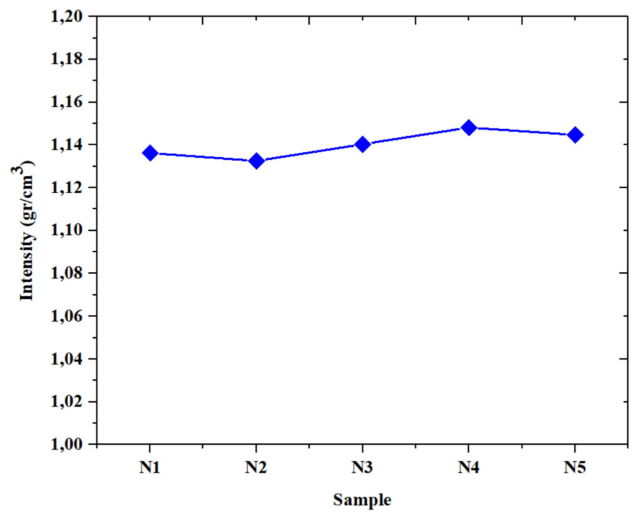

phase, its relatively lower hardness compared to chromium carbide imposes a limitation on the overall hardness of the composite [11, 26]. Therefore, the observed increase in hardness in the N2 sample is associated with the dominant effect of the reinforcement phase, while the slight reduction in density may result from inhomogeneous phase distribution or the presence of localized voids. When the Cr_3C_2 content was further increased to 9% and 12%, the density values increased again; however, a decreasing trend in hardness was observed. This behavior is likely related to the reduced Ni content, which compromised matrix continuity and weakened the interfacial bonding between the reinforcement and the matrix. Moreover, the agglomeration or non-uniform dispersion of Cr_3C_2 particles, along with the formation of microcracks, promoted intergranular fracture in the cermets. Although the observed increase in density at these compositions can be linked to the higher volumetric content of ceramic phases, the formation of localized voids and interfacial defects led to reduced fracture resistance. This outcome highlights that higher density does not necessarily indicate lower porosity and that localized microstructural defects can significantly influence the mechanical performance. In the sample with 18% Cr_3C_2 addition, both density and hardness decreased again. This reduction is believed to stem from the inability of the Ni binder phase to adequately wet or melt, thereby failing to fill the voids formed by the excess Cr_3C_2 particles. Consequently, at high reinforcement levels, the integrity of the microstructure was impaired, adversely affecting the mechanical properties. The thermal expansion coefficients of Cr_3C_2 and Ni are 10.3×10^{-6}/°C and 13×10^{-6}/°C, respectively. The matching of these thermal expansion coefficients effectively prevents the formation of interface microcracks and supports the interfacial bonding between ceramic and metallic phases. The growth of ceramic particles and pores within the structure and their inability to be removed have led to a decrease in density [1, 34, 39]. These results provide significant insights for determining the optimal addition ratio of Cr_3C_2 and for optimizing the microstructure and mechanical properties of Ni-based cermets. Figure 3 shows OM images of the samples before wear, taken at different magnifications.

The optical microscope examination of Ni-based cermets for microstructural characterization was conducted with images obtained at 200× and 500× magnifications. These optical microscope images are crucial for determining the distribution of Cr_3C_2 within the nickel matrix and the morphology of the phases. The images at 200× magnification reveal a homogeneous distribution of Cr_3C_2 particles within the Ni matrix. At this magnification, the sizes and shapes of the particles are clearly discernible. Specifically, samples with lower Cr_3C_2 content exhibit finer and more uniform particle distribution. This homogeneous distribution is thought to contribute to the improvement of the cermet's mechanical properties. The optical microscope images at 500× magnification reveal detailed microstructural features of the Cr_3C_2 particles. At this higher magnification, the interfaces between Cr_3C_2 particles and the nickel matrix become more distinct, allowing for the detection of potential microcracks and voids at the interfaces. Such microstructural examinations are critical for assessing the thermal and mechanical durability of cermets. As shown in Fig. 3, Cr_3C_2 particles are well-bonded to the matrix and exhibit a uniform distribution in the microstructure. Additionally, an increase in Cr_3C_2 content correlates with an increase in particle density and size. Particularly in samples with 9% and 12% Cr_3C_2 addition, the density and size of the particles have increased, although this has led to a decrease in hardness. These results highlight the importance of controlling the distribution of Cr_3C_2 within the Ni matrix. The homogeneous distribution of Cr_3C_2 particles and the quality of the interface bonding directly affect the mechanical and thermal performance of the cermets. The increase in Cr_3C_2 content led to a measurable rise in the overall density of the samples, as shown in the density measurements presented in Fig. 2, indicating a reduction in porosity. This correlation is supported by the microstructural observations presented in Fig. 3; as the Cr_3C_2 content increases, a noticeable decrease in porosity is observed. Particularly in the high-magnification SEM images (Fig. 3—500×), internal porosity is more clearly defined, and a reduction in both pore size and number is evident from samples N1 to N5. These visual findings corroborate the quantitative density measurements (Fig. 2) and reinforce the conclusion that the addition of Cr_3C_2 enhances the structural integrity of the material by reducing porosity. Furthermore, this improvement in structural integrity is also reflected in the

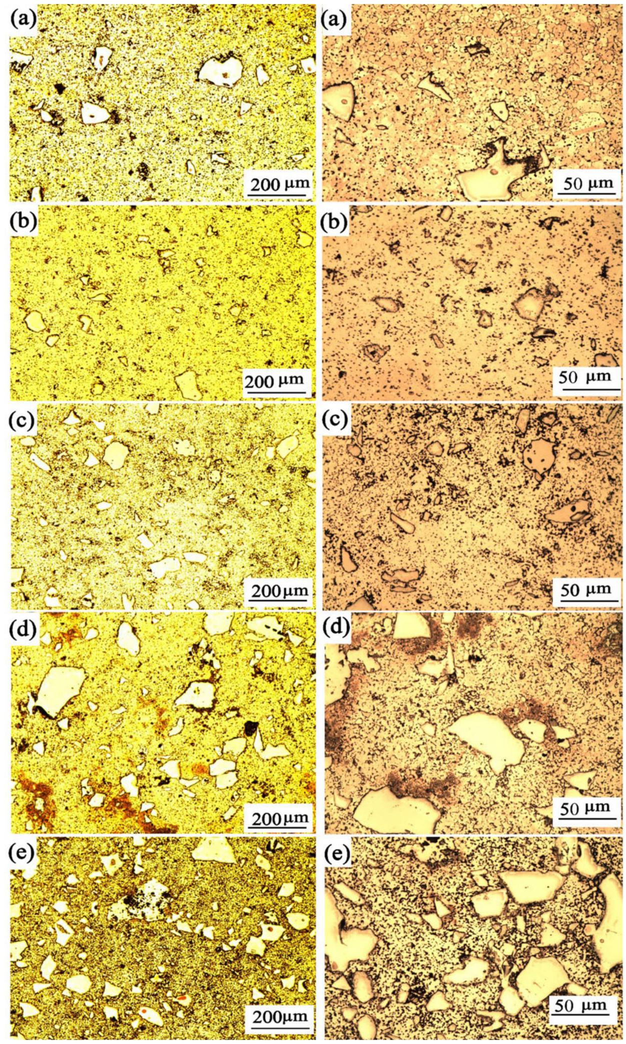

Fig. 3 OM images of the samples before wear (×200–×500): **a** Ni-3% Cr_3C_2, **b** Ni-6% Cr_3C_2, **c** Ni-9% Cr_3C_2, **d** Ni-12% Cr_3C_2, and **e** Ni-18% Cr_3C_2

microhardness measurements shown in Fig. 1, where an overall increase in hardness is observed in correlation with the increasing Cr_3C_2 content and decreasing porosity. Figure 4 shows the XRD pattern of Cr_3C_2–Ni samples processed at 960 °C under 35 MPa pressure for 6 min.

The examinations revealed that the produced samples contained three distinct phases: Cr_3C_2, Cr_7C_3, and surface-coincident cubic Ni [11, 35, 36]. The phases thought to belong to the peaks obtained from the XRD analysis graph were determined with the help of literature. A slight carbon loss was observed due to the sintering atmosphere not being an absolute vacuum and some of the Cr_3C_2 phase transforming into the Cr_7C_3 phase. This finding is consistent with results previously reported in the literature [10, 31, 35]. During high-temperature processing, partial dissolution of chromium and carbon from the added Cr_3C_2 particles into the Ni matrix occurs due to the high solubility and diffusion rates of these elements in Ni. As a result of carbon depletion and chromium enrichment in the matrix, the thermodynamically more stable Cr_7C_3 phase precipitates. This phase transformation from Cr_3C_2 to Cr_7C_3 is facilitated by the elevated temperature and the ability of the Ni matrix to act as a solvent for both Cr and C, promoting dissolution–reprecipitation mechanisms. Similar transformations of chromium carbides under comparable conditions have been reported in Ni-based systems. The transformation of Cr_3C_2 to Cr_7C_3 occurs depending on the solubility of the reinforcement and the cooling rate. Although the Cr_7C_3 phase can exhibit superior performance under high-temperature and wear conditions, this transformation is undesirable in a Ni-based material due to the dissolution of chromium from Cr_3C_2. The dissolution of chromium carbides leads to the formation of the Cr_7C_3 phase in the Ni matrix, and the presence of this phase can negatively impact the material's mechanical and thermal properties. The solubility of the Cr_3C_2 phase triggers the formation of Cr_7C_3 in the Ni matrix, which, although it may increase wear resistance, can adversely affect overall performance. In this context, the amount of Cr_3C_2 reinforcement and the sintering conditions should be carefully controlled to ensure the optimal performance of Ni-based cermets. The dry sliding wear behavior of the samples was investigated under a 10 N load against a 6-mm-diameter Al_2O_3 ball with a 300 m sliding distance, and the results are shown in Fig. 5. Figure 6 displays the graph of friction force variation with respect to the distance after the wear test applied to the cermets.

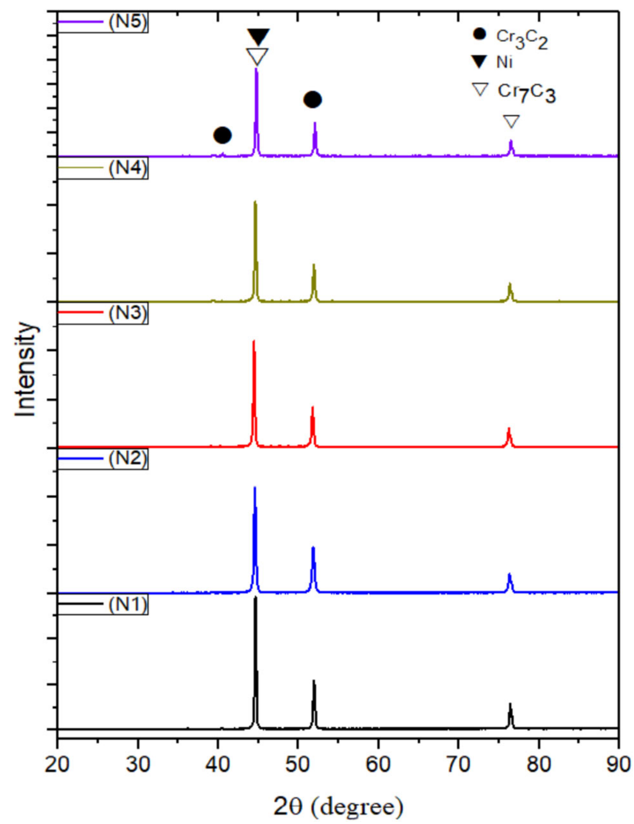

Fig. 4 XRD pattern of Cr_3C_2–Ni samples processed at 960 °C under 35 MPa pressure for 6 min

The N5 sample with 18% Cr_3C_2 content exhibits the highest density and hardness values, while the N1 sample with 3% Cr_3C_2content shows the lowest values. The microstructure of the chromium carbide ceramic particles used as reinforcement in the material is observed to be hexagonal and tetragonal in shape. An increase in the amount of reinforcement is associated with a noticeable increase in the frequency of these structures. The wear marks on the material's surface are in the form of parallel groove lines, indicating that the surface roughness of the material is being abraded by the hard particles during the friction process, and the wear mechanism occurring in the material is abrasive wear [37–40]. Additionally, the wear marks on the N1 sample with 3% Cr_3C_2 (Fig. 5a) are observed to be more pronounced. This is attributed to the low amount of reinforcement. As the amount of reinforcement increases, the carbide particles become more distinct. During the wear process, heating of the material surfaces occurs due to friction. At high temperatures, the loss of some particle boundaries leads to the merging and growth of ceramic particles. This results in larger carbide particles with an increase in their quantity (Fig. 5d) [1]. With the increase in chromium carbide content, the carbide-nickel cermets exhibited numerous voids (Fig. 5d). The formation of oxides (chromium oxide, nickel oxide) at the temperature of the wear test plays a lubricating role during the friction process. The variability in the wear marks on the samples is due to the partial differences in the oxide layer [37]. The oxides formed as a result of the wear process did not cover the material surface completely, leading to the removal of some oxides and the formation of relatively loose, shallow pits. Additionally, due to the alternating compressive contact with the abrasive ball and fatigue, material loss occurred on the oxide film of the material surface, resulting in noticeable cracks and spalling pits on the wear marks. The lower wear depth of the sample with 3% Cr_3C_2 compared to the sample with 18% Cr_3C_2, despite the latter having the highest Cr_3C_2 content, is attributed to the ease of sliding facilitated by the oxide layer on the sample surface. The lubricating effect of the oxide layer is greater due to the higher Cr_3C_2 content, which leads to increased wear depth. Figure 7 shows that weight loss observed in specimens as a function of reinforcement ratio.

In Cr_3C_2-reinforced nickel-based composites, the calculation of weight loss before and after wear was performed by multiplying the wear tracks on the material with the volume losses associated with these tracks. Wear tracks are a significant indicator that directly reflects the wear resistance of the material. The study observed a marked change in wear tracks with an increase in Cr_3C_2 content. Specifically, samples containing 6% and 12% Cr_3C_2 showed an expansion in wear tracks and a corresponding increase in weight loss. These findings indicate that increasing the Cr_3C_2 content up to a certain level positively affects wear resistance, but exceeding this level results in a reduction in wear resistance. At 18% Cr_3C_2 content, it was observed that wear tracks were the widest and this resulted in the highest weight loss (27.67 g). These results indicate that an excessive amount of Cr_3C_2 addition makes the material more brittle and more susceptible to wear, rather than enhancing its wear resistance. The increase in wear tracks is considered to be related to various microstructural factors, such as the distribution of chromium carbide particles within the nickel matrix, inter-phase bonding strength, and potential microstructural changes [38, 40].

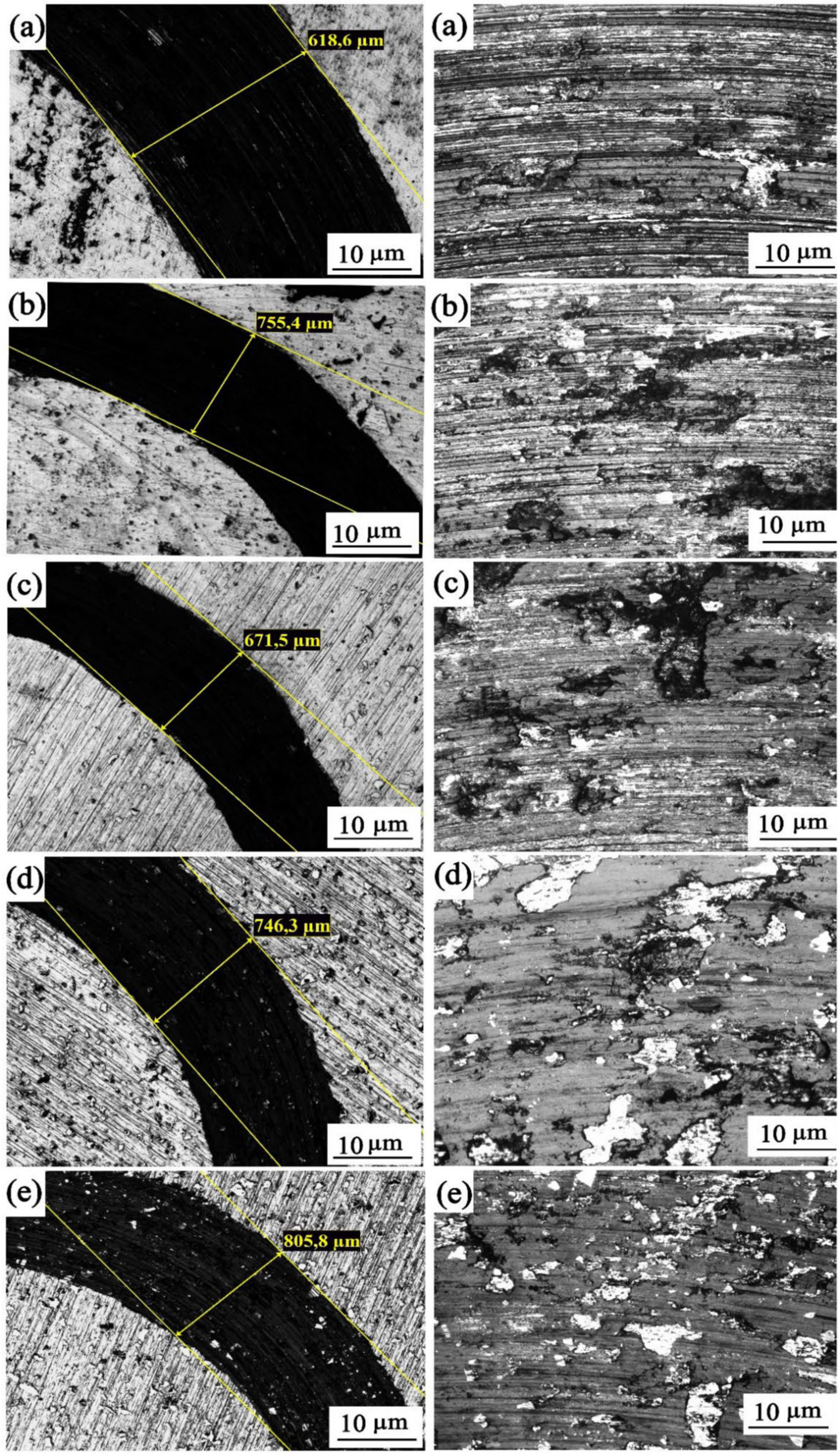

Fig. 5 Optical images of the cermets after the wear test at × 200 magnification: **a** Ni-3% Cr_3C_2, **b** Ni-6% Cr_3C_2, **c** Ni-9% Cr_3C_2, **d** Ni-12% Cr_3C_2, and **e** Ni-18% Cr_3C_2

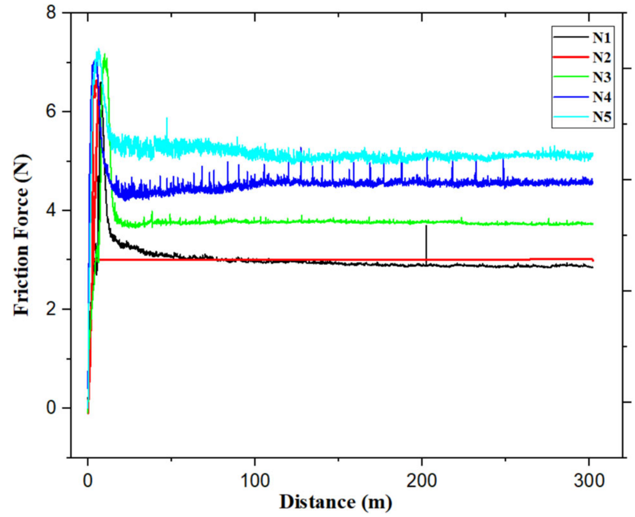

Fig. 6 The graph of friction force variation with respect to the distance after the wear test applied to the cermets

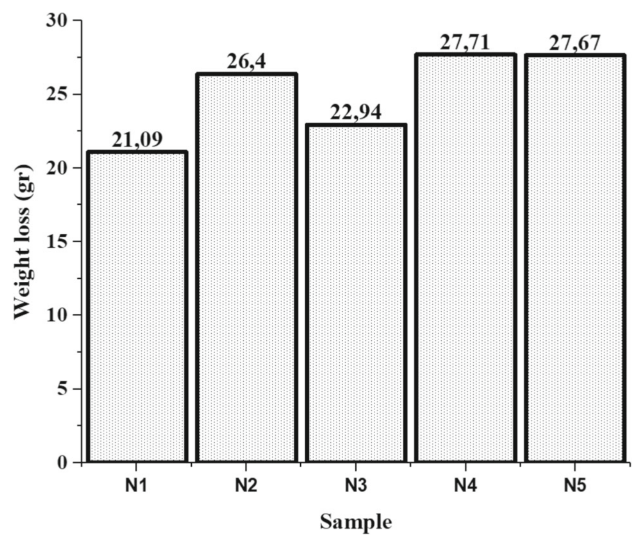

Fig. 7 The weight loss graph observed depending on the reinforcement ratio in the samples

4 Conclusions

This study evaluated the effects of Cr_3C_2 reinforcement on the microstructure and mechanical properties of Ni-based cermets. The research revealed that samples with different Cr_3C_2 contents exhibited significant differences in density, microhardness, and wear resistance.

- Samples with 18% Cr_3C_2 content were observed to have the highest microhardness values and the lowest density values, while samples with 3% Cr_3C_2 content exhibited the opposite trend.
- Samples with 3% Cr_3C_2 content showed fewer and more irregularly shaped carbide particles, whereas samples with 18% Cr_3C_2 content exhibited larger and more uniformly distributed carbide particles.
- The parallel groove markings on the wear tracks indicate that the surface roughness of the material was ground down during the wear process and addressed by the hard particles. These observations confirm the presence of an abrasive wear mechanism in the samples.
- Wear tests revealed that the oxide layers formed on the surface significantly influenced the wear resistance of the samples.
- The observed low wear depth in samples produced by powder metallurgy with 3% Cr_3C_2 is related to the effect of the binder powder used during the production process and the resulting oxide layer. This low Cr_3C_2 content facilitates a reduction in wear depth by creating a type of lubrication effect during friction due to the oxide layer, which helps to ease sliding. The oxide layer forms on the surface due to oxidation during the powder metallurgy process and the influence of the binder powders, and this layer plays a role in reducing wear under friction conditions.
- Higher microhardness values were observed in samples containing 18% Cr_3C_2. This high Cr_3C_2 content results in a denser carbide phase and, consequently, a harder microstructure. However, this may increase the thickness and hardness of the oxide layer, which can lead to greater depth formation on the surface during wear. Due to the influence of binder powders and the oxide layer, high

Cr_3C_2 content may enhance the wear resistance of the sample, but this phenomenon can also be associated with increased wear depths. These results indicate that the powder metallurgy method and the binder powders used have a significant impact on the surface properties.

Author contributions BT contributed to writing—review and editing, writing—original draft, validation, methodology, investigation, data curation. İS contributed to supervision, methodology, and investigation. EB contributed to writing—original draft and validation.

Funding Open access funding provided by the Scientific and Technological Research Council of Türkiye (TÜBİTAK). There is no funding source available.

Data availability The data supporting this study's findings are available from the corresponding author upon reasonable request.

Declaration

Conflict of interest The authors declare that they have no known competing financial interests or personal relationships that could have appeared to influence the work reported in this paper.

References

1. W. Zhai, B. Pu, L. Sun, H. Dong, Y. Wang, H. Lin, Y. Gao, Influence of Ni content on the microstructure and mechanical properties of chromium carbide-nickel composites. Ceram. Int. **46**, 8574–8760 (2020). https://doi.org/10.1016/j.ceramint.2019.12.114
2. Y. Lei, E. Wu, Sintering characteristics and microstructure of WC-Co-VC/Cr_3C_2 ultra fine cemented carbides. Rare Met. **28**, 482–486 (2009). https://doi.org/10.1007/s12598-009-0093-4
3. K. Jia, T.E. Fischer, B. Gallois, Microstructure, hardness and toughness of nanostructured and conventional WC–Co composites. Nanostruct. Mater.. Mater. **10**, 875–891 (1998). https://doi.org/10.1016/S0965-9773(98)00123-8
4. K. Kaunisto, M. Kotilainen, M. Karbu, J. Lagerbom, T. Vuorinen, M. Honkanen, M. Vippola, E. Turunen, The effect of carbon and nickel additions on the precursor synthesis of Cr_3C_2–Ni nano powder. Ceram. Int. **44**, 9338–9346 (2018). https://doi.org/10.1016/j.ceramint.2018.02.146
5. F. Weng, H. Yu, C. Chen, K. Wan, High-temperature oxidation behavior of Ni-based superalloys with Nb and Y and the inter face characteristics of oxidation scales. Surf. Interface Anal. **47**, 362–370 (2014). https://doi.org/10.1002/sia.5718
6. H. Kim, I. Shon, J. Yoon, J. Doh, Z. Munir, Rapidsintering of ultrafine WC-Ni cermets. Int. J. Refract Metal Hard Mater. **24**, 427–431 (2006). https://doi.org/10.1016/j.ijrmhm.2005.07.002
7. A. Zikin, I. Hussainova, C. Katsich, E. Badisch, C. Tomastik, Advanced chromium carbide-based hard facings. Surf. Coat. Technol. **206**, 4270–4278 (2012). https://doi.org/10.1016/j.surfcoat.2012.04.039
8. W. Chen, H. Shi, H. Xin, N. He, W. Yang, H. Gao, Friction and wear properties of Si_3N_4-hBN ceramic composites using different synthetic lubricants. Ceram. Int. **44**, 16799–16808 (2018). https://doi.org/10.1016/j.ceramint.2018.06.113
9. T. Sahraoui, N. Fenineche, G. Montavon, C. Coddet, Structure and wear behaviour of HVOF sprayed Cr_3C_2-NiCr and WC-Co coatings. Mater. Des. **24**, 309–313 (2003). https://doi.org/10.1016/S0261-3069(03)00059-1
10. K. Juhani, J. Pirso, S. Letunovits, M. Viljus, Phase evolution, microstructurecharacteristics and properties of Cr_3C_2–Ni cermets prepared by reactive sintering. Int. J. Mater. Prod. Technol. **40**, 75–91 (2011). https://doi.org/10.1504/IJMPT.2011.037207
11. C. Duran, S. Eroglu, Liquid-phase sintering and properties of Cr_3C_2/NiCrcermets. J. Mater. Process. Technol. **74**, 69–73 (1998). https://doi.org/10.1016/S0924-0136(97)00251-3
12. J. Pirso, M. Viljus, S. Letunovits, K. Juhani, Reactive carburizing sintering: a novel production method for high quality chromium carbide-nickel cermets. Int. J. Refract Metal Hard Mater. **24**, 263–270 (2006). https://doi.org/10.1016/j.ijrmhm.2005.06.002
13. I. Hussainova, J. Pirso, M. Antonov, K. Juhani, S. Letunovits, Erosion and abrasion of chromium carbide basedcermets produced by different methods. Wear **263**, 905–911 (2007). https://doi.org/10.1016/j.wear.2006.12.027
14. I. Hussainova, I. Jasiuk, M. Sardela, M. Antonov, Micromechanical properties and erosive wear performance of chromium carbide based cermets. Wear **267**, 152–159 (2009). https://doi.org/10.1016/j.wear.2008.12.104
15. L. Sun, W. Hui, L. Xu, W. Zhai, H. Dong, Y. Wang, L. He, J. Peng, Interface characterization and mechanical properties of Mo-added chromium carbide-nickel composite. Ceram. Int. **46**, 27071–27079 (2020). https://doi.org/10.1016/j.ceramint.2020.07.184
16. F. Deorsola, D. Vallauri, G. OrtigozaVillalba, B. Benedetti, Densification of ultrafine WC-12Co cermets by pressure assisted fast electric sintering. Int. J. Refract Metal Hard Mater. **28**, 254–259 (2010). https://doi.org/10.1016/j.ijrmhm.2009.10.007
17. S. Dosta, G. Bolelli, A. Candeli, L. Lusvarghi, I. Cano, J. Guilemany, Plastic deformation phenomena during cold spray impact of WC-Coparticles onto metal substrates. Acta Mater. Mater. **124**, 173–181 (2017). https://doi.org/10.1016/j.actamat.2016.11.010
18. W. Zhang, X. Zhang, J. Wang, C. Hong, Effect of Fe on the phases and microstructure of TiC-Fe cermets by combustion synthesis/quasi-isostatic pressing. Mater. Sci. Eng. A **381**, 92–97 (2004). https://doi.org/10.1016/j.msea.2004.04.026
19. S. Ordonez, L. Carvajal, V. Martinez, C. Agurto, J. Marin, L. Olivares, I. Iturriza, Fracture toughness of SiC-Cu based alloys cermets. Mater. Sci. Forum **498–499**, 350–356 (2005). https://doi.org/10.4028/0-87849-984-9.350
20. M.R. Akbarpour, Tensile properties and fracture characteristics of nano structured copper and Cu-SiC nanocomposite produced by mechanical milling and spark plasma sintering process. J. Mater. Eng. Perform. **27**, 1987–1994 (2018). https://doi.org/10.1007/s11665-018-3267-0
21. W. Zhai, Y. Gao, L. Sun, Y. Wang, K. Niwa, M. Hasegawa, High pressure in-situ synthesis and physical properties of Cr_3C_2–Ni cermets. Ceram. Int. **43**, 17202–17205 (2017). https://doi.org/10.1016/j.ceramint.2017.09.145
22. Y. Ding, T. Hussain, D. McCartney, High-temperature oxidation of HVOF thermally sprayed NiCr–Cr_3C_2 coating: microstructure and kinetics. J. Mater. Sci. **50**, 6808–6821 (2015). https://doi.org/10.1007/s10853-015-9238-z

23. Z. Marcano, J. Lesage, D. Chicot, G. Mesmacque, E. Puchi-Cabrera, M. Staia, Microstructure and adhesion of Cr_3C_2–NiCr vacuum plasma sprayed coatings. Surf. Coat. Technol. **202**, 4406–4410 (2008). https://doi.org/10.1016/j.surfcoat.2008.04.017
24. M. Detroye, F. Reniers, Synthesis and characterization of chromium carbides. Appl. Surf. Sci. **120**, 85–93 (1997). https://doi.org/10.1016/S0169-4332(97)00228-6
25. A. Klenk, M. Speicher, K. Maile, Weld behavior of martensitic steels and Ni-based alloys for high temperature components. Procedia Eng. **55**, 414–420 (2013). https://doi.org/10.1016/j.proeng.2013.03.273
26. E. Bullock, M. McLean, D.E. Miles, Creepbehaviour of a Ni–Ni_3Al–Cr_3C_2 eutectic composite. Acta Metall. **25**, 333–344 (1977). https://doi.org/10.1016/0001-6160(77)90152-3
27. K. Gong, T.B. An, Z.F. Zhou, Z.L. Tian, C.H. Li, Study on wear behaviors of Ni_3Al/Cr-carbides cladding layer on high strength steel substrate. Adv. Mater. Res. **936**, 1273–1282 (2014). https://doi.org/10.4028/www.scientific.net/AMR.936.1273
28. K. Gong, Z. Zhou, P.W. Shum, H. Luo, Z. Tian, C. Li, Tribologicalevaluation on Ni_3Al-based alloy and its composites under unlubricated wear condition. Wear **270**, 195–203 (2011). https://doi.org/10.1016/j.wear.2010.10.060
29. K. Gong, H. Luo, D. Feng, C. Li, Wear of Ni_3Al-based materials and its chromwium-carbide reinforced composites. Wear **265**, 1751–1755 (2008). https://doi.org/10.1016/j.wear.2008.04.038
30. S. Kumar, T. Raghu, P. Bhattacharjee, G. Rao, U. Borah, Strain rate dependent microstructural evolution during hot deformation of a hot isostatically processed nickel base superalloy. J. Alloys Compd. **681**, 28–42 (2016). https://doi.org/10.1016/j.jallcom.2016.04.185
31. J.C. Chang, C. Choi, J.C. Kim, Y.H. Yun, Development of microstructure and mechanical properties of a Ni-bases ingle-crystal superalloy by hot-isostatic pressing. J. Mater. Eng. Perform. **12**, 420–425 (2003). https://doi.org/10.1361/105994903770342953
32. B. Ruttert, C. Meid, L.M. Roncery, I. Lopez-Galilea, M. Bartsch, W. Theisen, Effect of porosity and eutectics on the high temperature low-cycle fatigue performance of a nickel-basesingle-crystalsuperalloy. Scripta Mater. **155**, 139–143 (2018). https://doi.org/10.1016/j.scriptamat.2018.06.036
33. W. Xuan, X. Zhang, Y. Zhao, J. Li, B. Wang, X. Ren, Z. Ren, Mechanism of improved intermediate temperature plasticity of nickel-base single crystal superalloy with hot isostatic pressing. J. Mater. Res. Technol. **14**, 1609–1617 (2021). https://doi.org/10.1016/j.jmrt.2021.07.010
34. M. Demirel, V. Koç, Analysing the microstructures and pin-on-discwear properties of 1010 steel-based and B_4C-added materials produced through powder metallurgy. World J. Eng. Technol. **9**, 682–707 (2021). https://doi.org/10.4236/wjet.2021.93047
35. W. Zhai, Y. Gao, L. Sun, Y. Xiao, L. He, Y. Wang, Effect of molybdenum addition on the microstructure and mechanical properties of Cr_3C_2-20 wt.% Ni cermet. Mater. High Temp. **34**, 272–278 (2017). https://doi.org/10.1080/09603409.2017.1312089
36. W. Zhai, Y. Gao, L. Sun, L. He, Y. Wang, Improvement of high temperature oxidation behavior of Cr_3C_2–20 wt %Ni cermets by adding 1 wt % Mo. J. Alloys Compd. **731**, 271–278 (2018). https://doi.org/10.1016/j.jallcom.2017.10.012
37. J. Du, F. Li, Y. Li, H. Lu, X. Qi, B. Yang, C. Li, P. Yu, J. Wang, L. Gao, The influence of nano-CeO_2 on tribological properties and microstructureevolution of Cr_3C_2-NiCrCoMo composite coatings at high temperature. Surf. Coat. Technol. **428**, 127913 (2021). https://doi.org/10.1016/j.surfcoat.2021.127913
38. R.M. Kumar, H. Kumar, G. Harmain, S. Albert, Wearperformance of Ni-Cr-B-Si hardfacecoatingsfabricated by cold metal transfer welding. Proc. Inst. Mech. Eng. C J. Mech. Eng. Sci. **236**, 1850–1860 (2022). https://doi.org/10.1177/09544062211023085
39. E. Kaya, S. Buytoz, Influence of borides on microstructure and mechanical properties of a Ni alloy. Mater. Test. (2024). https://doi.org/10.1515/mt-2023-0425
40. E. Kaya, M. Ulutan, E. Çakır, S. Buytoz, Influence of post heat treatment on tribological and microstructural properties of plasma wire arc additive manufactured maraging steels. Mater. Test. (2024). https://doi.org/10.1515/mt-2024-0273